



# Derivation and validation of metrics for breast cancer screening from diffuse optical tomography imaging data

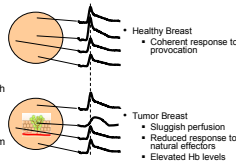
R.L. Barbour<sup>1,2</sup>, H.L. Graber<sup>1,2</sup>, Y. Pei<sup>2</sup>, Y. Xu<sup>1,2</sup>, D.C. Lee<sup>1</sup>, M.S. Katz<sup>3</sup>, N. Patel<sup>4</sup>, K. Jagarlamudi<sup>5</sup>, O.R. Nwaguma<sup>6</sup>, and W.B. Solomon<sup>7</sup>

<sup>1</sup>SUNY Downstate Medical Center; <sup>2</sup>NIRx Medical Technologies LLC; <sup>3</sup>Drexel University College of Medicine; <sup>4</sup>Kaiser Permanente; <sup>5</sup>The Brooklyn Hospital Center; <sup>6</sup>Pennsylvania State University; <sup>7</sup>Maimonides Medical Center

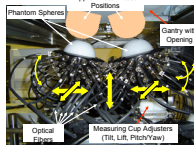


## Introduction

- Dynamic Near Infrared Optical Tomography (DYNOT)
  - Provides measures of relative concentrations of hemoglobin (Hb)
  - Oxygenated, deoxygenated, total
  - Noninvasive functional imaging *in vivo*
  - Exogenous contrast agents not required
- Growth of solid tumors frequently accompanied by:
  - Marked changes in the vascular supply sustaining tumor growth
  - State of impaired perfusion
  - Relatively hypoxic environment
- To image the preceding, we developed:
  - A dual-breast diffuse optical tomography (DOT) imaging system
  - Capable of simultaneous bilateral measurements



## Measuring Head (1st-Generation) for Simultaneous Dual-Breast Imaging



- DYNOT simultaneous dual-breast measuring head
  - Each optical fiber (31 per breast) is both source and detector for NIR light
  - Data collected from 124 channels (62 fibers x 2 wavelengths) in parallel
  - Sources location is time-multiplexed
- Measurement rate: 2 complete image frames (to 8x10<sup>4</sup> data points) per second

## Physiological Hypotheses

- There are mechanisms by which a cancerous tumor's "volume of influence" may be appreciably larger than the tumor itself
  - This is a consequence of well-characterized differences between vasculature in cancerous solid tumors, and in healthy tissue (or in non-cancer pathologies)
- A key to increasing diagnostic power is comparing detector and image data between the two simultaneously examined breasts
  - Vascular responses under automatic control should be similar in the two breasts
  - Responses under local control (e.g., autoregulation) also should be similar, if both breasts are healthy
- If one breast has a cancerous tumor, and the other doesn't, what macroscopic differences could we expect?
  - Increased amplitudes for vasomotor rhythms, in the tumor-bearing breast (TBB)
  - Owing to hypoxic environment of many solid tumors
  - Greater temporal correlation across the breast volume, and greater spatial homogeneity, in the tumor-free breast (TFB)
  - Abnormal response, in the TBB, to events that stress the microvasculature
- Therefore, three categories of diagnostic metrics will be considered in the clinical study
  - Each is devised to reveal one of the three types of expected difference between the TBB and TFB
  - Group 1:** Indices of resting vasomotion amplitude
    - Computed from resting-state measurement data
    - Are sensitive to enhanced vasomotion, possibly associated with tumor angiogenesis
  - Group 2:** Index of spatially coordinated dynamics
    - Computed from resting-state measurement data
    - Is sensitive to differences in timing of blood delivery within each breast
  - Group 3:** Measures of pressure-induced blood volume and oxygenation shifts
    - Computed from data collected during Valsalva maneuver
    - Are sensitive to venous congestion and delayed reperfusion, which can lead to tumor hypoxia
    - In the TBB, compared to the contralateral TFB, one would expect to see:
      - Increased oxygen desaturation of Hb
      - Increased blood volume change
      - Increase in time needed for recovery

## Clinical Study Design

### 1. Subject population

- Retrospective – subjects whose data is used for derivation of breast-cancer diagnostic metrics
- Prospective – subjects whose data is used for testing and validation

Subject Group	Breast Pathology Status	N	Age (yr) [mean ± SD]	BMI (kg-m <sup>2</sup> ) [mean ± SD]	Tumor Size [largest dimension]	Clinical Description
Retrospective	Active CA	14	47.9 ± 12.3	28.7 ± 5.3	10 × 3 cm 4 > 3 cm	10 ductal carcinoma 1 ductal & lobular carcinoma 1 mucinous carcinoma 1 metastatic CA 1 inflammatory CA 4 Grade 2/3 Grade 2: 1 had no biopsy data
	Prior CA	3	50.7 ± 9.4	30.4 ± 0.5	—	All had lumpenectomies 2-3 yr prior to NIRS study
	Pre-CA	0	—	—	—	—
Non-CA Pathology	Non-CA Pathology	11	45.7 ± 5.6	28.7 ± 5.5 (N=7)	—	3 fibrocystic disease 4 breast cyst 1 axillary cyst 2 benign breast lumps 1 breast reduction surgery
	No History of Breast Pathology	9	41.6 ± 10.0	30.3 ± 7.2	—	—
	Active CA	14	51.4 ± 10.9	30.4 ± 4.5	5 ≤ 3 cm 9 > 3 cm	13 ductal carcinoma 1 axillary adenocarcinoma with primary duct ectasia and hyperplasia 3 Grade 2, 11 Grade 3 3 prior ductal carcinoma 1 prior mucinous carcinoma All had lumpenectomies 2-6 yr prior to NIRS study
Prospective	Prior CA	4	60.8 ± 9.3	25.5 ± 1.7	—	2 DCIS 1 atypical ductal hyperplasia 1 extremely dense breasts
	Pre-CA	4	53.5 ± 3.4	29.0 ± 4.1 (N=3)	—	2 fibrocystic changes 1 benign breast lump 1 breast reduction surgery
	Non-CA Pathology	6	43.7 ± 8.4	26.6 ± 4.9 (N=4)	—	1 cystic disease 2 fibrocystic changes 1 benign breast lump 1 breast reduction surgery
No History of Breast Pathology	8	44.0 ± 6.8	30.5 ± 8.9	—	—	

Subject Group	n <sub>i</sub>	Mean	SD	Range	n <sub>j</sub>	Mean	SD	Range	
Active Breast Cancer (CA)	Retrospective / Training Group	14	47.9	12.3	29-70	14	28.7	5.3	21.6-43.9
	Prospective / Validation Group	14	51.4	10.9	37-71	14	30.4	4.5	22.7-38.1
Non-CA	Retrospective / Training Group	23	44.7	8.6	26-62	19	30.1	6.1	18.4-44.4
	Prospective / Validation Group	22	48.7	10.0	30-69	18	28.2	6.6	21.2-48.5

### 2. Analysis of dual-breast DOT image time series

- 4-D (volume + time) data sets are reduced to the following scalar values:

Experimental Condition	Tumor-Associated Phenotype	Scalar Metric
Breast Density	Angiogenesis	1. $SMRSD = \frac{\sum_{i=1}^N \sum_{j=1}^N  r_{ij}(t) }{N}$
		2. $SSD7SD = \frac{\sum_{i=1}^N \sqrt{\sum_{j=1}^N  r_{ij}(t) ^2} - SMRSD}{N}$
		3. $TMSSD = \frac{\sum_{i=1}^N \sum_{j=1}^N  r_{ij}(t)  \cdot \sum_{k=1}^N  r_{ik}(t) }{N}$
		4. $7SDM = \frac{\sum_{i=1}^N \sum_{j=1}^N  r_{ij}(t) }{N}$
		5. $7SDSSD = \frac{\sum_{i=1}^N \sqrt{\sum_{j=1}^N  r_{ij}(t) ^2} \cdot \sum_{k=1}^N  r_{ik}(t) }{N}$
Spatial Coordination	Hypoxia	6. $SC(L) = \frac{1}{N} \frac{\sum_{i=1}^N \sum_{j=1}^N  r_{ij}(L)  \cdot \sum_{k=1}^N  r_{ik}(L) }{\sum_{i=1}^N \sum_{j=1}^N  r_{ij}(L) }$ where $r_{ij}(L) = M(r_{ij}, L)$ (Complex Morlet wavelet decomposition) $M(r_{ij}, L) = \int_{-\infty}^{\infty} r_{ij}(t) e^{i2\pi f t} dt$ (normalized to unit mean value, in the frequency bands of interest) $M(r_{ij}, L) = \int_{-\infty}^{\infty} r_{ij}(t) e^{i2\pi f t} dt$ (Average over the image volume)
		7. $A = \frac{\sum_{i=1}^N \sum_{j=1}^N  r_{ij}(t)  \cdot \sum_{k=1}^N  r_{ik}(t)  \cdot \sum_{l=1}^N  r_{il}(t) }{\sum_{i=1}^N \sum_{j=1}^N  r_{ij}(t)  \cdot \sum_{k=1}^N  r_{ik}(t) }$

- Differences between metric values, for each subject's two breasts, are calculated as:
  - Tumor minus non-tumor for training-set cancer subjects
  - Left minus right for training-set non-cancer subjects, and for validation-set subjects
- Each metric is converted into six candidate diagnostic parameters, by normalizing the inter-breast difference in a variety of ways:
  - Difference divided by larger, smaller, or average value of the two individual-breast values
  - Difference multiplied by larger, smaller, or average of the individual-breast values

### 2. Analysis of dual-breast DOT image time series [continued]

- Assessment of sensitivity, specificity, positive and negative predictive values
  - Univariate: parametric and nonparametric tests for difference between means of CA and non-CA subgroups of the training set
  - Multivariate: binary logistic regression (BLR)
    - Use leave-out-one cross-validation (LOOCV) to determine sensitivity to idiosyncrasies of the training-set subjects
    - Validate the predictors that are most successful with respect to the retrospective group, by applying them to the data for the prospective group
- Aggregates (averages) for 1 or more multivariate predictors
  - The overall number of aggregates is  $2^{C_1} + 2^{C_2} + 2^{C_3} + \dots + 2^{C_{21}} + 2^{C_{22}} = 4,194,303$
  - For each subject, the aggregate breast-cancer probability is the average of the separate probabilities according to the multivariate predictors
  - For sensitivity and specificity calculations, a breast-cancer probability of 0.5 is taken as the diagnostic threshold

## Results

### 1. Diagnostic accuracy for multivariate predictors

- As determined by BLR-LOOCV computations, these had statistically highly significant discriminatory ability and robustness
- Predictors 1-13 are hypothesis-based, physiological premises (above) guided the selection of which univariate metrics to include
- Predictors 14-22 are data-driven: a backward-elimination algorithm was used to determine which combinations of univariate features were the "best" multivariates, without regard to biological significance

Multivariate Predictor	Hb <sub>ret</sub>	Hb <sub>pro</sub>	Hb <sub>diff</sub>	Sensitivity, Ret. (%)	Specificity, Ret. (%)	Sensitivity, Pro. (%)	Specificity, Pro. (%)
1	1.5	1.5	0.5	94.3	95	74.5	93.7
2	1.3	1.5	4.5	78.6	90	64.3	60
3	6	6	6	90	90	85.7	93.3
4	7.8	7.8	1.5	100	100	71.2	92.3
5	2.9	6	1	85.7	99	87.1	86.7
6	1.6	6	1	71.4	90	87.1	93.3
7	1.3	5.6	1.3	85.7	95	78.6	100
8	1.3	5.6	1.3	100	90	78.6	100
9	1.8	3	3	90	90	78.6	92.3
10	6	6	8	90	90	71.4	84.6
11	8	5.6	8	80	90	71.4	92.3
12	6	8	1	90	81.8	64.3	84.6
13	2.8	4.8	1.3	90	90	64.3	76.9
14	3	6	6	90	90	64.3	93.3
15	3	6	6	57.1	95	57.1	100
16	8	9	9	90	90	71.4	84.6
17	7.8	6	6	80	90	71.4	84.6
18	3	3	21.6	90	90	85.7	100
19	3.5	6	4	100	95	78.6	93.3
20	8	6	8	80	81.8	64.3	84.6
21	4	3	9	90	90	57.1	61.5
22	6	6	6	90	90	71.4	84.6

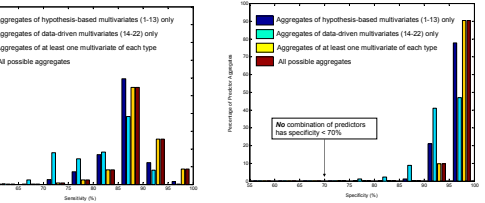
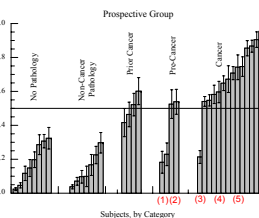
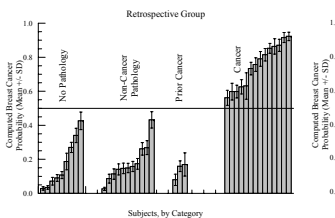
† The Difference/Maximum formulation is used for these predictors, and Difference/Maximum for all the others

### 3. Average breast-CA probability, for each subject, across the 196,639 highly successful aggregates

- Low-grade DCIS, and previously diagnosed DCIS not confirmed upon re-exam
- High-grade DCIS, and dense, cystic breasts
- Small (< 1 cm) tumor, near the chest wall
- Adenocarcinoma in axillary lymph node
- Lumpectomy 8 yr. prior to NIRS exam, relapse 1 yr. after NIRS exam

### 4. Correlations between computed breast-CA probability and demographic variables: age and BMI

- Only the No Pathology and Non-CA Pathology sub-groups were considered here
- Results are suggestive of a trend, in all cases, but sample size is too small for statistical significance



## Conclusions

- Prospective-group results show that the derived multivariate metrics do operate on features of the image data that are related to breast-cancer status, and not to any idiosyncratic properties of the retrospective group.
- The observation that the inter-breast differences have the predicted directionality implies that our assumptions, regarding the effects of tumor development and growth on the dynamic properties of the vasculature, are largely correct
- The successful application of metrics derived by spatial integration of DOT image data implies that the vascular correlates of tumor growth and development are present over a volume that extends a substantial distance beyond the histological margins of the tumor.
- The preceding conclusions, plus the suggestive results from preliminary examination of the trends between breast-CA probability and age or BMI, indicate that the relationships between the DOT metrics and other data types (demographics, histology, tumor-receptor findings) should be more fully explored (NIH01-104).